Stable wide-angle Fourier-finite difference downward extrapolation of 3-D wavefields

Biondo Biondi, Stanford University

SUMMARY

I derive an unconditionally stable implicit finite-difference operator that corrects the constant-velocity phase shift operator for lateral velocity variations. My method is based on the Fourier Finite-Difference (FFD) method first proposed by Ristow and Ruhl (1994). Contrary to previous results, my correction operator is stable even when the reference velocity is higher than the medium velocity, and in presence of sharp contrasts in velocities. Because of this additional capability, I can apply a frequency-dependent interpolation after the correction step, that significantly reduces the residual phase error after interpolation, the frequency dispersion caused by the discretization of the Laplacian operator, and the azimuthal anisotropy caused by splitting.

INTRODUCTION

As 3-D prestack wave-equation imaging becomes practically possible, we need robust, efficient, and accurate methods to downward continue 3-D wavefields. In particular, wide-angle methods are crucial for prestack imaging, because at least one of the paths connecting the image point in the subsurface to the source/receiver locations at the surface is likely to propagate at a wide angle.

Fourier methods, such as phase shift (Gazdag, 1978), handle wide-angle propagation efficiently and accurately, but only for vertically layered media. In contrast, finite-difference methods can easily handle lateral velocity variations, but are not efficient for wide-angle propagation. A natural strategy thus combines a Fourier method with a finite-difference method to derive an extrapolation method that enjoys the strengths of both. This is not a new idea, and indeed the first proposed adaptations of Fourier methods, Phase Shift Plus Interpolation (PSPI) (Gazdag and Sguazzero, 1984) and split-step (Stoffa et al., 1990), can be interpreted as being zero-order finite-difference corrections to a phase shift extrapolator. Ristow and Ruhl (1994) first proposed a genuinely finite-difference correction to phase shift, which they dubbed Fourier Finite-Difference (FFD). It employs implicit finite differences (Claerbout, 1985) to handle lateral velocity variations. Pseudo-screen propagators (Jin et al., 1998), wide-angle screen propagators (Xie and Wu, 1998), generalized-screen propagators (Le Rousseau and de Hoop, 1998), and local Born-Fourier migration (Huang et al., 1999), are related methods that have been recently proposed in the literature.

It can be easily shown that the FFD correction is more accurate than other methods that employ implicit finite-difference (Biondi, 2000), such as pseudo-screen propagators (Jin et al., 1998) and wide-angle screen propagators (Xie and Wu, 1998). Because the computational complexity of the three methods is comparable, the FFD correction is therefore more attractive than the others, and it is the focus of my paper. Unfortunately, when the original FFD method is applied in presence of sharp discontinuities in the velocity model (e.g. unsmoothed salt bodies) it can generate numerical instability. Stability is a necessary condition for a migration method to be practically useful. The stable FFD correction that I present in this paper overcomes the instability problems related to the original FFD method. To derive a stable version of the FFD correction, I adapted the bullet-proofing theory developed by Godfrey et al. (1979) and Brown (1979) for the 45-degree equation. The bullet-proofed FFD correction is unconditionally stable for arbitrary variations in the medium velocity *and* in the reference velocity. Further, I demonstrate that it is unconditionally stable when the medium velocity is either higher *or* lower than the reference velocity. This is a useful result, and differs with a statement in Ristow and Ruhl's paper, that asserts their method to be unstable when the medium velocity is lower than the reference velocity. The stability of the new FFD correction, even when the reference velocity is higher than the medium velocity and has lateral variations, makes it a suitable building block for the construction of a new wide-angle downward continuation algorithm that is efficient and accurate in 3-D. At each depth step, the wavefield is propagated with $N_{v_{\rm r}}$ reference velocities using phase shift, where $N_{v_{\rm r}}$ is determined according to both the range of velocities in the current depth slice and the maximum propagation angle that we need for accurate imaging of the events of interest. Then, the $N_{v_{\rm r}}$ reference wavefields are combined to create two wavefields: one for which the reference velocity is lower than the medium velocity, the other one for which the reference velocity is higher than the medium velocity. A stable FFD correction is applied to both wavefields, and the corrected wavefields are linearly interpolated with frequency-dependent weights. The frequency-dependent interpolation enables a significant reduction of the frequency dispersion introduced by the discretization of the Laplacian operator in the implicit finite difference step.

In 3-D, the FFD corrections can be efficiently applied by splitting. The algorithm that I propose suffers much less from azimuthal anisotropy caused by splitting than did the original FFD method. The phase errors as a function of azimuth have opposite behavior when the differences between the reference velocity and medium velocity have opposite signs. Therefore, these phase errors tend to cancel each other when the two wavefields are interpolated after the FFD correction.

STABLE FOURIER-FINITE DIFFERENCE CORRECTION

The FFD correction is based on a direct expansion of the difference between the phase-shift operator evaluated at the medium velocity v and at the reference velocity $v_{\rm r}$. The downward-continued wavefield is approximated as

$$P_{z+\Delta z} = P_z e^{i k_z^{v} \Delta z} = P_z e^{i k_z^{v_{\rm r}} \Delta z + i \frac{\Delta k_z}{\Delta s} \Delta s \Delta z}, \qquad (1)$$

where $\Delta k_z / \Delta s$ is approximated by continued fractions as

$$\frac{\Delta k_z}{\Delta s} \approx \omega \left[1 + \frac{\frac{v_{\rm r} v X^2}{2}}{1 - \frac{\left(v_{\rm r}^2 + v^2 + v_{\rm r} v\right) X^2}{4}} \right]. \qquad (2)$$

An implicit finite-difference implementation of the FFD correction as expressed in equation (2) is stable for smooth velocity variations. But numerical instability may develop when there are sharp discontinuities in the velocity field (Biondi, 2000).

In constant velocity, the correction operator is unitary (all-pass filter) because its eigenvalues have zero imaginary part. Numerical instability originates when variations in the velocities terms multiplying the second derivative $[v_{\rm r} v X^2$ and $\left(v_{\rm r}^2 + v^2 + v_{\rm r} v\right) X^2]$ cause the imaginary part to become different from zero. To assure that this does not happen, we first rewrite equation (2) as

$$\frac{\Delta k_z}{\Delta s} \Delta s \approx \omega \left[\frac{(v_{\rm r} - v)}{v_{\rm r} v} + \frac{2 {\rm sign}(v - v_{\rm r}) |v_{\rm r} - v|}{v_{\rm r}^2 + v^2 + v_{\rm r} v} \frac{\frac{\left(v_{\rm r}^2 + v^2 + v_{\rm r} v\right) X^2}{4}}{1 - \frac{\left(v_{\rm r}^2 + v^2 + v_{\rm r} v\right) X^2}{4}} \right]. \qquad (3)$$

Then we rewrite $\left(v_{\rm r}^2 + v^2 + v_{\rm r} v\right) X^2$ as the product of a matrix with its adjoint, that is,

$$\Sigma^{'} X^2 \Sigma = - \frac{1}{\omega^2 \Delta x^2} \Sigma^{'} D^{'} D \Sigma \qquad (4)$$

where D is a causal finite-difference approximation of the first derivative and

$$\Sigma = \frac{1}{2}\text{Diag}\begin{bmatrix} \sqrt{{}_1v^2 + {}_1v_r{}^2 + {}_1v\ {}_1v_r} \\ \vdots \\ \sqrt{{}_{i-1}v^2 + {}_{i-1}v_r{}^2 + {}_{i-1}v\ {}_{i-1}v_r} \\ \sqrt{{}_iv^2 + {}_iv_r{}^2 + {}_iv\ {}_iv_r} \\ \sqrt{{}_{i+1}v^2 + {}_{i+1}v_r{}^2 + {}_{i+1}v\ {}_{i+1}v_r} \\ \vdots \\ \sqrt{{}_nv^2 + {}_nv_r{}^2 + {}_nv_nv_r} \end{bmatrix}, \qquad (5)$$

where ${}_iv_r$ and ${}_iv$ are respectively the reference velocity and medium velocity at the i grid horizontal location.

The matrix $\Sigma^{'}X^2\Sigma$ is now guaranteed to have real eigenvalues. Because both I and $\Sigma^{'}X^2\Sigma$ are normal matrices that can be diagonalized by the same similarity transformation (Brown, 1979), the matrix $\left(I + \Sigma^{'}X^2\Sigma\right)^{-1}\Sigma^{'}X^2\Sigma$ is also guaranteed to have real eigenvalues.

Notice that the sign of the velocity perturbations was isolated in equation (3). It is possible to demonstrate that the new FFD correction is guaranteed to be stable independently from the value of $\text{sign}(v - v_r)$, as long the sign is constant (Biondi, 2000).

The reference velocity v_r and the medium velocity v can be interchanged at will in the previous development without changing the stability conditions. Therefore, the stable FFD correction is not only stable in presence of sharp discontinuities in the medium velocity, but also in presence of sharp discontinuities in the reference velocity. This property is exploited in the next section, for the design of an efficient and accurate interpolation scheme.

The new FFD correction can be easily implemented using an implicit finite-difference scheme, such as Crank-Nicolson. However, in 3-D, an implicit scheme would imply the solution of a linear system with a banded matrix with much wider band than that in 2-D. The cost of the exact 3-D solution would be thus considerably higher than the 2-D solution, because the cost of banded-matrix solvers is proportional to the width of the band. To reduce computational cost, a splitting algorithm (Jakubowicz and Levin, 1983) can be employed. The stability of a splitting algorithm derives directly from the analysis above, since splitting consists of the successive application of the FFD correction along the two horizontal coordinate axes. In the next section I discuss how the capability of using both positive and negative velocity corrections yields a significant improvement in the accuracy of the splitting algorithm.

THE FOURIER FINITE-DIFFERENCE PLUS INTERPOLATION (FFDPI) ALGORITHM

The stable FFD correction developed in the previous section has the desired characteristics for being used as the main building block of an efficient and accurate wide-angle downward continuation algorithm. To achieve accuracy, we can interpolate between wavefields that have been phase shifted with several reference velocities, and corrected by the stable FFD method. In theory, arbitrary accuracy can be achieved by an increase in the number of reference velocities. The structure of the algorithm is similar to the PSPI method (Gazdag and Sguazzero, 1984) and the extended split-step method (Kessinger, 1992), except that a wide-angle correction (FFD) is employed instead of a narrow-angle one (vertical shift). This improvement reduces the errors over the whole range of propagation angles.

Two results reached in the previous section are important for the definition of a stable and accurate interpolation scheme. First, the stability of the FFD correction is independent of the sign of the velocity perturbation to be applied, as long as the sign is constant within the same correction step. This result enables a *linear interpolation* between a wavefield corresponding to reference velocities lower than the medium velocity, and a wavefield corresponding to reference velocities higher than the medium velocity. Previously, because of the requirement for the reference velocity to be lower than the medium velocity, only a *nearest-neighborhood interpolation* was possible when multiple velocities were used in conjunction with wide-angle corrections (Huang et al., 1999). Second, the reference velocity can vary at will laterally, without compromising the stability of the method. Because of these results, it is sufficient to apply the FFD correction only twice at each depth step, and thus computations can be saved. The first correction would be applied to a wavefield constructed from all the reference wavefields computed with a reference velocity lower than the medium velocity. The second one would be applied to a wavefield constructed from all the reference wavefields computed with a reference velocity higher than the medium velocity. To decrease the effects of frequency dispersion on the interpolated wavefield, the interpolation weights can be easily made frequency dependent. Because the Fourier Finite-Difference method and interpolation are both fundamental components of the new method, I will refer to it as Fourier Finite-Difference Plus Interpolation method, or FFDPI. It is important to notice that the stability analysis developed in the previous section strictly applies only to the simple FFD correction, not to its combination with an interpolation scheme like FFDPI. In theory, when FFDPI is used, instability can still develop as it does for PSPI (Margrave and Ferguson, 1999). However, the possibility for the FFDPI algorithm to become unstable is mostly theoretical and does not represent a real practical limitation.

FFDPI error analysis

The most important advantage of the FFDPI algorithm is a drastic reduction of the propagation errors achieved when the wavefields that have been downward continued with multiple reference velocities are linearly interpolated. The errors are very small for all propagation angles up to the angle corresponding to the steepest wave that is non-evanescent with the reference velocity higher than the medium velocity.

Figure 1 compares the relative phase errors measured as a function of the propagation angle, for split step, FFD, FFDPI, and Split Step Plus Interpolation (SSPI). The medium velocity v is equal to 2 km/s, and two reference velocities are assumed: one 10% lower than the medium velocity (1.8 km/s), the other one 10% higher than the medium velocity (2.2 km/s). The interpolation weights were computed to zero the errors at 64 degrees. The temporal frequency of the wavefield was assumed to be zero. The FFDPI error is contained within the ± 1% band and is considerably lower than both the simple FFD and the SSPI errors. As expected, both the FFDPI and the SSPI curves show a zero crossing at 64 degrees.

Numerical dispersion severely degrades the accuracy of the simple FFD correction at high frequency, as is evident in the impulse responses shown in Figures 2 and 3. In contrast, by using frequency-dependent weights we can greatly reduce the effects of numerical dispersion and maintain the accuracy advantages of FFDPI over SSPI. Figure 4 shows the impulse after applying FFDPI with frequency dependent weights. It should be compared with the impulse responses shown in Figures 2 and 3.

Azimuthal anisotropy

A recurring problem that hampers the application of implicit finite-difference methods to 3-D wave extrapolation is the azimuthal anisotropy associated with splitting (Jakubowicz and Levin, 1983). Of course, this problem affects also the FFD correction applied by splitting

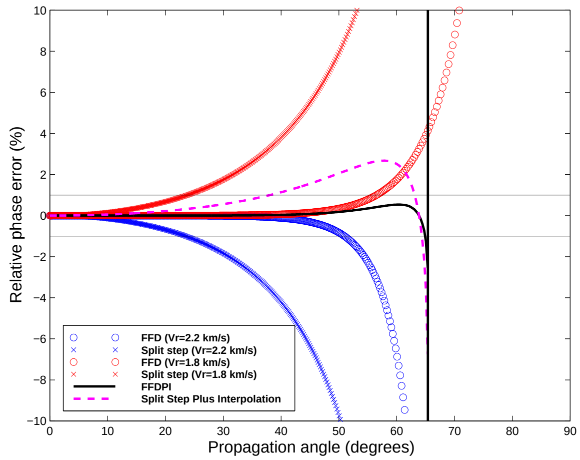

Figure 1: Relative phase-error curves assuming v=2 km/s and starting from two reference velocities (v_r^-=1.8 km/s and v_r^+=2.2 km/s), for split step, FFD, FFDPI and Split Step Plus Interpolation (SSPI). The temporal frequency of the wavefield was assumed to be zero. The vertical solid line indicates the maximum propagation angle (65.4 degrees) when v_r=2.2 km/s and v=2 km/s. The horizontal solid lines indicate the 1% phase error level.

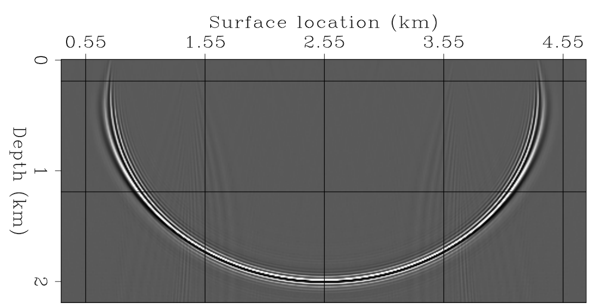

Figure 2: Impulse response after FFD correction, with reference velocity equal to 1.8 km/s and medium velocity equal to 2 km/s. The maximum frequency in the data is 42 Hz and the spatial sampling is 10 m in both directions.

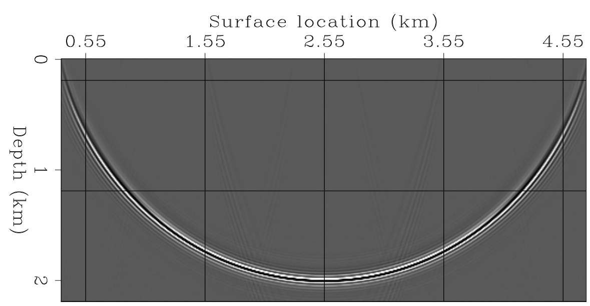

Figure 3: Impulse response after FFD correction, with reference velocity equal to 2.2 km/s and medium velocity equal to 2 km/s. The maximum frequency in the data is 42 Hz and the spatial sampling is 10 m in both directions.

(Cockshott and Jakubowicz, 1996). However, I will show that for the FFDPI algorithm the azimuthal anisotropy is greatly reduced without recurring to sophisticated linear solvers.

Figure 5 compares relative phase errors as a function of the azimuth measured for a propagation angle of 61 degrees. The frequency-dependent interpolation weights were computed to zero the phase error along an azimuthal direction oriented at 22.5 degrees with respect to the inline/crossline axes, and at a dip angle of 61 degrees ($\theta_0 = 61°$). The azimuthal direction of 22.5 was chosen because it is the midpoint between the two extrema of the error curves. As in the previous figures, the medium velocity v is equal to 2 km/s, and two reference velocities are assumed: one 10% lower than the medium velocity (1.8 km/s), the other one 10% higher than the medium velocity (2.2 km/s). The plots show the phase errors at two frequencies (0 Hz and 100 Hz) for the FFDPI algorithm, the FFD correction starting from the lower reference velocity, and the FFD correction starting from the higher reference velocity. Notice that for both the simple FFD correction cases the azimuthal anisotropy decreases as the frequency increases, though the average phase error increases as well. But the crucial, and useful, feature of the phase errors function for the FFD corrections, is that the azimuthal variations are in the opposite directions when the differences between the reference velocity and medium velocity have opposite signs. Consequently, the phase error of the interpolation method is contained within the ± 1% band and it is much lower than the error of either of the simple FFD corrections. At higher frequencies (100 Hz) the impulse response of FFDPI is almost perfectly isotropic.

The theoretical analysis is confirmed by the characteristics of the impulse responses. Figure 6 is the merge of two impulse responses along the inline direction cut at a depth that corresponds to a propagation angle of 64.2 degrees, that is close to the maximum propagation angle (65.4 degrees) for the high reference velocity (2.2 km/s). For negative values of the in-line coordinate, the plot shows the depth slice for the exact impulse response. For positive values of the in-line coordinate, the plot shows the depth slice for the impulse response obtained by FFDPI. It is evident that the result of the interpolation scheme is almost perfectly isotropic and is only slightly dispersive.

CONCLUSIONS

The combination of Fourier methods' accuracy for wide-angle propagation with implicit finite differences' flexibility for modeling lateral velocity variations yields accurate and efficient downward-propagation methods. The FFD correction is the most attractive among several methods that employ implicit finite-difference to correct constant-velocity phase shift for lateral velocity variations. However, the correction operator originally presented by Ristow and Ruhl (1994) can be unstable in the presence of sharp discontinuities in the velocity function. In this paper I present and successfully test an unconditionally stable version of the FFD correction. The stable version has computational complexity similar to that of the potentially unstable one.

Using the stable FFD correction as a building block, I derive an accurate and stable wide-angle migration (Fourier-Finite Difference Plus Interpolation). The FFDPI algorithm is based on the interpolation of two wavefields corrected with the FFD method, with opposite signs of the velocity perturbations. This interpolation step compensates for both the azimuthal anisotropy and the frequency-dispersion of the simple FFD corrections.

The accuracy and the cost of FFDPI algorithm can be easily controlled by setting the number of reference velocities. Small phase errors can be achieved across the whole range of propagation angles, from zero to the limit determined by the evanescent limit for the reference velocity above the true medium velocity. The method is thus particularly attractive when high accuracy is needed for the downward continuation operators, as in prestack depth migration below salt bodies.

ACKNOWLEDGMENTS

I thank the sponsors of the Stanford Exploration Project (SEP) for supporting the research presented in this paper. This research was also partially funded by the ACTI project # 4731U0015-3Q.

REFERENCES

Biondi, B., 2000, Stable wide-angle fourier-finite difference downward extrapolation of 3-D wavefields: submitted to Geophysics.

Brown, D., 1979, Muir's rules for matrices: Another look at stability: SEP–**20**, 125–142.

Claerbout, J. F., 1985, Imaging the Earth's Interior: Blackwell Scientific Publications.

Cockshott, I., and Jakubowicz, H., 1996, 3-D migration using the Fourier finite-difference method: 66th Annual Internat. Mtg., Soc. Expl. Geophys., Expanded Abstracts, 435–438.

Gazdag, J., and Sguazzero, P., 1984, Migration of Seismic Data by Phase-Shift Plus Interpolation: Geophysics, **49**, no. 2, 124–131.

Gazdag, J., 1978, Wave equation migration with the phase-shift method: Geophysics, **43**, no. 10, 1342–1351.

Godfrey, R. J., Muir, F., and Claerbout, J. F., 1979, Stable extrapolation: SEP–**16**, 83–87.

Huang, L. J., Fehler, M. C., and Wu, R. S., 1999, Extended local Born Fourier migration method: Geophysics, **64**, no. 5, 1524–1534.

Jakubowicz, H., and Levin, S., 1983, A simple exact method of three-dimensional migration – Theory: Geophys. Prosp., **31**, no. 1, 34–56.

Jin, S., Wu, R. S., and Peng, C., 1998, Prestack depth migration using a hybrid pseudo-screen propagator: 68th Annual Internat. Mtg., Soc. Expl. Geophys., Expanded Abstracts, 1819–1822.

Kessinger, W., 1992, Extended split-step Fourier migration: 62th Annual Internat. Mtg., Soc. Expl. Geophys., Expanded Abstracts, 917–920.

Le Rousseau, J. H., and de Hoop, M. V., 1998, Modeling and imaging with the generalized screen algorithm: 68th Annual Internat. Mtg., Soc. Expl. Geophys., Expanded Abstracts, 1937–1940.

Margrave, G., and Ferguson, R., 1999, An explicit, symmetric wavefield extrapolator for depth migration: 69th Annual Internat. Mtg., Soc. Expl. Geophys., Expanded Abstracts, 1461–1464.

Ristow, D., and Ruhl, T., 1994, Fourier finite-difference migration: Geophysics, **59**, no. 12, 1882–1893.

Stoffa, P. L., Fokkema, J. T., de Luna Freire, R. M., and Kessinger, W. P., 1990, Split-step Fourier migration: Geophysics, **55**, no. 4, 410–421.

Xie, X. B., and Wu, R. S., 1998, Improve the wide angle accuracy of screen method under large contrast: 68th Annual Internat. Mtg., Soc. Expl. Geophys., Expanded Abstracts, 1811–1814.

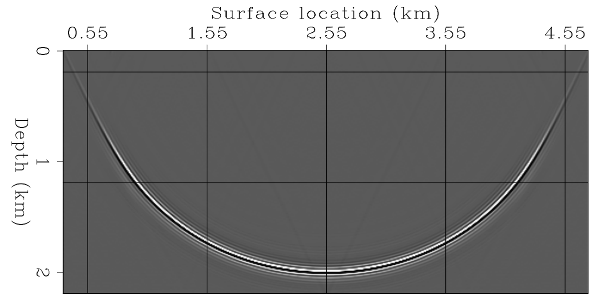

Figure 4: Impulse response after interpolation with frequency-dependent weights between a reference velocity equal to 1.8 km/s and a reference velocity equal to 2.2 km/s.

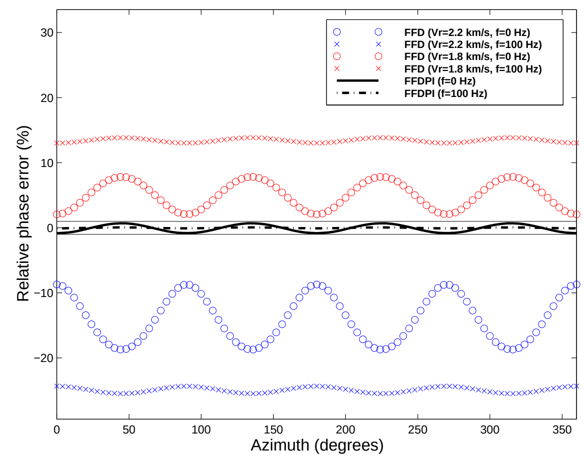

Figure 5: Relative phase-error curves for FFD and FFDPI, as a function of the azimuth. The medium velocity was assumed to be v=2 km/s and the two reference velocities were v_r^-=1.8 km/s and v_r^+=2.2 km/s. Two temporal frequencies of the wavefield were assumed: 0 Hz and 100 Hz. The horizontal solid lines indicate the ± 1% phase-error level.

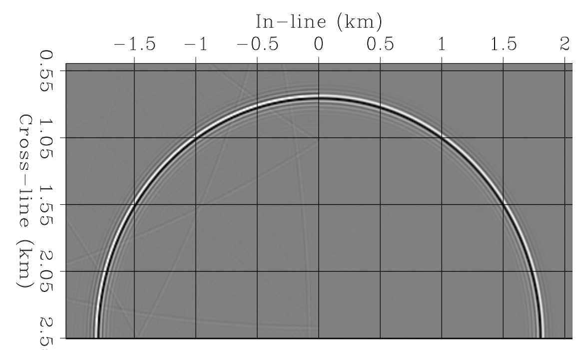

Figure 6: Depth slices through impulse responses: 1) left half corresponds to the exact impulse response with the medium velocity of 2 km/s, 2) right half corresponds to the FFDPI results.